Analysis of UV Photographs of the Shroud of Turin

Thomas McAvoy

Professor Emeritus, Institute for Systems Research, Department of Chemical and Biomolecular Engineering, and Bioengineering Department, University of Maryland, College Park MD, 20742, USA
mcavoy@umd.edu

Abstract: The Shroud of Turin is perhaps the most widely studied ancient relic in history. In this paper recently published uv photographs of the Shroud are analyzed. It is shown that the Shroud exhibits very unique uv fluorescence properties. It fluoresces more on its right side than its left side. Also, where comparisons can be made the Shroud fluoresces more on its dorsal side than its frontal side, and fluorescence is stronger near the center of the image on the Shroud than near the head or feet. These results are compared to conclusions from a published simulation of neutron irradiation of the Shroud.

1. Introduction

The Shroud of Turin is a unique linen cloth with an image of a crucified man on it. Many people believe that this cloth is Christ's burial shroud. The Shroud of Turin has been studied more than any other ancient relic in history. In 1976 two scientists, one of whom was John Jackson, put a photograph of the Shroud into a VP-8 analyzer and they found that amazingly the Shroud photo displayed 3 dimensional properties [1]. Intrigued by this interesting result the two scientists established a research project (Shroud of Turin Research Project, STURP) to investigate the Shroud image. Two years later with 29 other US scientists joining the project the team traveled to Turin to carry out a scientific analysis of the Shroud. In Turin the US group was joined by a number of international colleagues. The instrumentation used by the STURP team included among others equipment for x-ray transmission and fluorescence detection, microscopy, photoelectric spectrophotometry, infrared spectrometry and uv fluorescence, black and white, and color photography [2]. The STURP technical photography team took approximately one thousand documented, high quality images of the Shroud [3]. In April 2019 199 high quality photos taken by Vern Miller as a member of STURP were published on the web [4]. In this paper twenty two of Miller's uv fluorescence photos of the Shroud are examined in detail.

In 1988 three laboratories carried out radiocarbon dating of the Shroud [5]. The results of this dating gave a range of 1260 to 1390 indicating that the Shroud was a medieval cloth. The statistical analysis of the radiocarbon data carried out in [5] was subsequently questioned by van Haelst [6] who showed that the data contained a systemic bias. The portion of the Shroud tested was approximately 1.5 inches long by ¾ inch wide and yet the radiocarbon dates differed by over 200 years from one end of the sample to the other. All the radiocarbon dates should have been close to one another. Recently, Casabianca et al [7] carried out a thorough statistical analysis of the raw data that was collected during the 1988 radiocarbon dating study. It took a court order for this data to be released by the owner of the data, the British Museum. Casabianca et al [7] conclude that their statistical analysis reinforced the argument against the goodness of the radiocarbon dating of the Shroud, suggesting the presence of serious incongruities among the raw measurements. They further state that the measurements made by the three laboratories on the Turin Shroud sample suffer from a lack of precision which seriously affects the reliability of the 95% AD 1260–1390 interval. These authors recommend that additional testing be done on the Shroud. In contrast to the radiocarbon results essentially all other data on the Shroud indicate a much earlier origin. Recent research by Fanti et al using both FT-IR and Raman spectroscopy [8] and mechanical property testing [9] date the Shroud to Christ's time. Fanti et al's dating results are: FTIR 300 BC ± 400 yrs [8], Raman 200 BC ± 500 yrs [8], and mechanical testing 372 AD ± 400 yrs [9]. All three results are compatible with Christ's time.

Since the publication of the radiocarbon dating results a number of explanations for the dates based on the idea of contamination of the sample site used have been presented. In 1990 Harry Gove, who pioneered the mass spec method

used for the radiocarbon dating addressed this issue of contamination [10]. Gove states: "even if it did exist in the form of contemporary organic carbon, which is one way the apparent age can be reduced, 64% of the Shroud sample would have to be such contamination and only 36% of 2000-year-old carbon to change the measured date from the first century AD to the 14th century. Visible inspection by the author of the shroud sample received by Arizona before it was cleaned made it clear that no such gross amount of contamination was present." More recently Rucker [11] has provided a detailed discussion about why the carbon dating of the Shroud is not explained by normal contamination. Rucker's calculations indicate that anywhere from 60 to 80% of the carbon in the Shroud sample would have to come from contamination, and such a large amount would be easily visible if that were the case. Even though there are valid statistical questions about the radiocarbon dating results, the very large discrepancy between the medieval radiocarbon dates and the first century appears very likely to be due to another cause.

At present standard science cannot explain how the image on the Shroud was formed, and as a result other, controversial explanations have been put forward. Phillips in 1989 [12] hypothesized that a neutron flux could be the reason for the increase in radiocarbon in the Shroud. Rinaudo [13,14] worked on this hypothesis and expanded it to include a mechanism for formation of the Shroud image in addition to the change in the radiocarbon date. Rinaudo hypothesized that deuterium from the body split apart and emitted protons and neutrons. The neutrons caused the radiocarbon date change and the protons caused the image. In 1989 STURP scientist John Jackson first proposed his fall through hypothesis involving vacuum ultraviolet radiation from the body in the formation of the Shroud image [15]. Jackson's hypothesis predicted that there would be a doubly superficial image on the back of the Shroud associated only with the frontal image on the Shroud. When the Shroud backing was removed in 2002 for cleaning a faint image on the back of the Shroud behind the frontal image was observed in agreement with Jackson's prediction [16]. There was no double image on the dorsal side. In 2012 Antonacci [17] published a detailed paper based primarily on Jackson and Rinaudo's work on how particle radiation from the body could explain the Shroud's images and its carbon dating. Antonacci has also discussed these concepts in depth in his recent book on the Shroud [18]. These publications are controversial since a body does not normally emit radiation. However, as Antonacci discusses [17] the radiation hypothesis does explain all of the Shroud's 32 unique properties which he lists in his paper, including its 3 dimensional property. The neutron radiation hypothesis is testable if additional tests can be done on the Shroud itself [19]. Neutron radiation would have created very long-lived radioactive isotopes, e.g. Chlorine 36 (half-life 301000 yrs) and Calcium 41 (half-life 102000 yrs), at levels well beyond those that occur naturally. If these isotopes are found in the Shroud that would help support the neutron radiation hypothesis.

A very interesting follow up on the suggestion made by Phillips [12] that neutron radiation could have altered the radiocarbon content of the Shroud, and therefore its radiocarbon date, was carried out by Rucker [20]. He was interested in simulating whether neutrons emitted from the body could have altered the radiocarbon dating results. He used a computer software package [21], MCNP (Monte Carlo Neutron Particle) that was developed at the Los Alamos National Laboratory to simulate neutron emissions. Rucker developed a very detailed geometric model of a tomb that would have existed in the first century AD. Then he carried out extensive simulations using the MCNP software. Rucker's calculations showed that there would be a very wide range of radiocarbon dates if samples were taken from numerous areas on the Shroud. A very detailed description of Rucker's rationale, simulation method and results is given in his paper [20].

In this paper twenty two of the uv photos that Miller took in 1978 [4] are analyzed. A non-uniform illumination problem with these photos is discussed and a solution presented. The uv photos are cast into the CIE L*a*b color space [22] to get pixel intensity. It is shown that the Shroud exhibits very unique uv fluorescence intensity characteristics whereby its right side fluoresces more than its left side. Further where comparisons can be made the fluorescence from the dorsal side of the Shroud is stronger than fluorescence from the frontal side. Lastly fluorescence is stronger near the center of the image on the Shroud than near the image of the head or feet. The center of the image on the Shroud also fluoresces more than the sides of the Shroud near it. Rucker's MCNP simulation of neutron irradiation of the Shroud [20] exhibits very similar properties in terms of predicted radiocarbon dates. A comparison of the predictions of Rucker's MCNP simulation and the uv fluorescence properties of the Shroud is given, assuming that uv fluorescence is affected by neutron radiation. The paper concludes with suggestions for future research.

2. Illumination problem with Miller uv photos

In an earlier paper [23] McAvoy analyzed the uneven illumination problem with the uv photos taken by Miller in 1978. A brief review of this analysis is given here. Figure 1 shows the lighting configuration used by Miller for his uv photography [2].
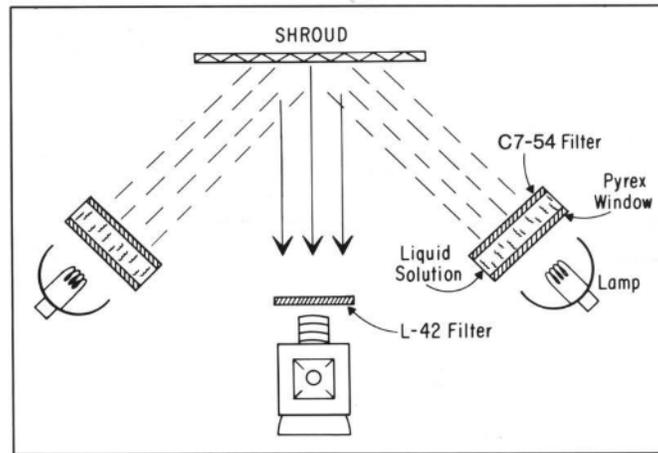

Fig. 1. Lighting configuration used by Miller for uv photography [2].

Two 200 watt lamps that had uv bandpass filters were used. These two lamps were focused at 45° on the region of the Shroud that was being photographed. The camera had a uv filter and it took photos at a 90° angle. Figure 2 shows a cropped version of one of Miller's uv photos (image 3d-UV-S1-E-12_0476) that was downloaded from the web [4].

Fig. 2. Cropped Miller image (3d-UV-S1-E-12_0476) [4] © Vernon Miller, 1978.

Figure 2 includes the area between the frontal and dorsal head images. Cropping and an additional discussion about how Miller took his uv photos are given below. The image in Figure 2 is different from the uv photo analyzed by McAvoy [23], but it can be used to demonstrate the uneven illumination problem with Miller's uv photos. Each pixel in the photo in Figure 2 can be converted from the Red, Green, Blue color space (RGB) to the CIE L*a*b color space [22]. Figure 3 shows a schematic of CIE L*a*b color space, which was designed to approximate human vision.

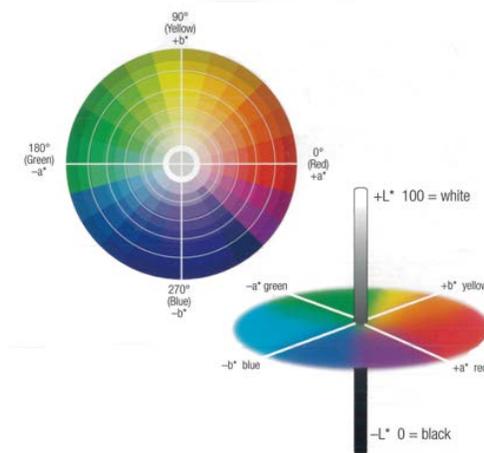Fig. 3. CIE L*a*b Color Space

The vertical L axis in the CIE L*a*b space gives image intensity, which is what is examined in this study. The two horizontal axes, a and b, give image color. MATLAB® and its Image Processing Toolbox [24] are used to analyze all the images in this study. The Image Processing Toolbox has a subroutine (rgb2lab) that allows one to convert an RGB image to a CIE L*a*b image. MATLAB® also has numerous statistical and plotting routines.

The MATLAB® function contour(Z,[10:60]) creates a contour plot containing the isolines of matrix Z, where Z contains intensity values L for each pixel in a uv photo. The pixel locations would be the matrix Z coordinates. The [10:60] range determines the colors displayed in the contour plot images. All contour plots in this paper use this range so that contour plots can be compared to one another. Figures 4 gives the contour plot for the intensity L of the uv image in Figure 2.
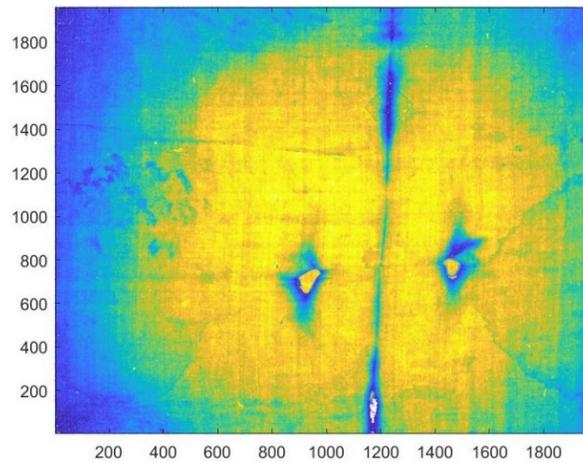

Fig. 4. Contour plot of CIE L*a*b intensity L for Fig. 2

The yellow/gold regions in Figure 4 are associated with the highest intensities, while the green regions have lower intensity, and the blue regions have the lowest intensity. The intensity in each of these colored regions is not constant but it varies. Figure 4 clearly shows the effects of the uv lighting configuration used by Miller and shown in Figure 1. McAvoy [23] examined a number of additional uv photos taken by Miller and they all exhibited the contour structure shown in Figure 4. Figure 4 and the other uv images analyzed demonstrate that the Shroud location being photographed was not evenly illuminated. The two lamps shown in Figure 1 focus more uv light on the middle of the area being photographed than on the periphery. However, the center of the image is not necessarily the center of where the uv

lights were focused. Figure 4 shows that there is more blue region to the left of the image than to the right. There is also more yellow region at the bottom of the image than at the top. A method to find the center of the uv illumination is discussed below. Avis el al [25] also pointed out the lack of uniform illumination in Miller's uv black and white Shroud images which they also analyzed.

3. First 16 uv photos analyzed

In [4] 16 of Vern Miller's uv photos are given under the titles: B and D UV light photos taken at burn areas at f:22 (f-number) at 8 seconds. The titles of these photos indicate that Miller was interested in focusing on the burn marks on the Shroud. This is probably the reason that the uv lights used were focused somewhat off the center point of each image. The 16 photos were downloaded and they cover the entire Shroud and except for one which is discussed below they all appear to have the same f-number and exposure time. The f-number of a camera lens is the ratio of the camera's focal length to the diameter of the entrance aperture. The f-number is a dimensionless number that is a quantitative measure of lens speed. Miller also used the same camera and film to take all of his photos. The grid layout used by Miller for the 16 photos [2] is shown in Figure 5, where the area that the image in Figure 2 came from is highlighted by a red rectangle.
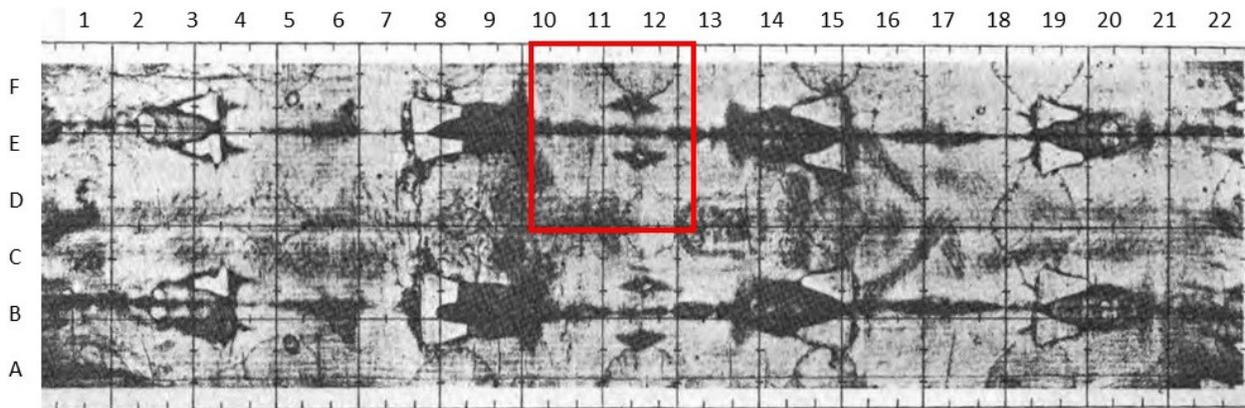

Fig. 5. Grid layout used by Miller for uv photography. Red rectangles shows where photo in Fig. 2 was taken [2].

Note that Miller's uv photos need to be rotated 90° counterclockwise to fit them into the grid shown in Figure 5. Eight of Miller's uv photos covered the A,B,C 1 to 22 portion of the grid and the other eight the D,E,F 1 to 22 portion.

References [2,3] give details about the photographic procedure followed by Miller when he took his STURP photos. He was particularly careful in taking these photos. In [3] the plan he used is discussed in detail where it is stated: "this plan involved careful attention to camera and film selection as well as considerable attention to the problems of obtaining a large number of accurately positioned (registered), focused and exposed images in an unknown (but assumed relatively short) period of time". As part of the plan Miller used a specially designed rail system shown in Figure 6 for all of his photos, including the uv photos.
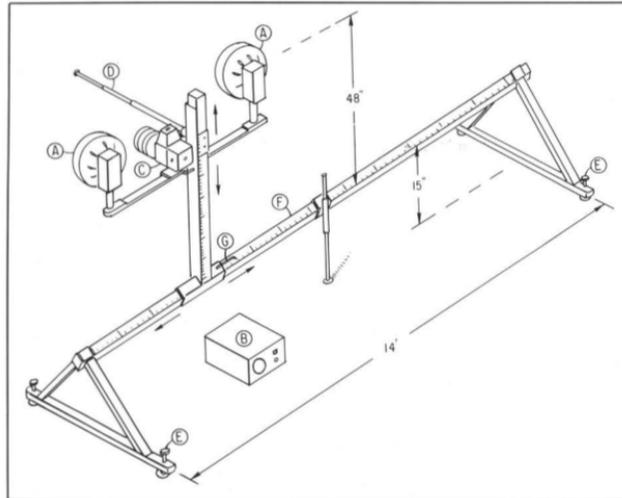
Fig. 6. Lighting and photographic rail system used by Miller for photography [2]

Item D in this figure is a telescoping rod that was fixed to keep the distance between the camera, C, and the Shroud constant for all photos. For the uv photography the lights, A, were turned to 45º angles as shown in Figure 1.

4. Preliminary treatment of uv photos

4.1 Resizing uv photos

To illustrate how the downloaded photos were resized to have an equal number of pixels the photo in Figure 2 is considered. The downloaded photo is shown in Figure 7.

Fig. 7. Uncropped image (3d-UV-S1-E-12_0476) [4] (Red Rectangle 1) © Vernon Miller, 1978.

This photo is reasonably detailed with a pixel size of 8176x6132. First the photo was cropped to eliminate the borders. The cropped photo has a pixel size of 5338x5398. All 16 uv photos have slightly different cropped pixel sizes. To speed up computer processing all 16 photos were resized to a common pixel size of 1962x1989. The final cropped image of Figure 7 is shown in Figure 2.

4.2 Finding the center of illumination

To facilitate comparing the uv images to one another it is important that the center of illumination be identified. Once identified then each image can be centered around the illumination center point and calculations of the properties of the image can be made and compared. For the centering method used the average column intensity of the contour plot in Figure 4 was calculated, and this intensity is shown Figure 8.
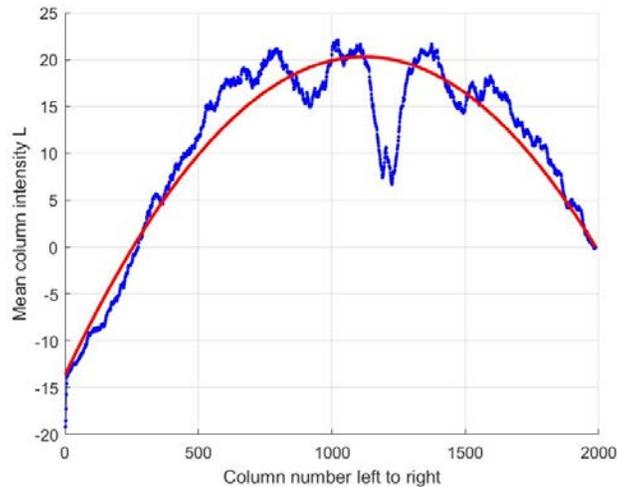

Fig. 8. Plot of Average column intensity L from CIE L*a*b plot in Fig. 4

For this plot the mean of the values of L at column 1989 was subtracted out so the plot ends at zero. The spikes in the plot are due to the burn marks in the image. A parabola which is symmetrical was fitted to the mean intensity and it is shown by the red line. The parabola crosses zero at a column value of 254. The region to the left of column 254 was cropped so that illumination was centered across the remaining columns. Next the rows in Figure 4 were treated. In order to use the mean function in MATLAB® on the rows Figure 4 had to be rotated 90º clockwise. After this rotation the region to be cropped is to the right. A plot the resulting mean row intensity is shown in Figure 9. The mean of the bottom row was subtracted from the intensity values so the plot starts at zero. A parabola was fitted to the data and the parabola crossed the zero line at 1781 on the x axis. Thus the top 1962-1781 = 181 rows were cropped. The resulting cropped image had a pixel size of 1782x1736. A contour plot for this cropped image is shown in Figure 10.
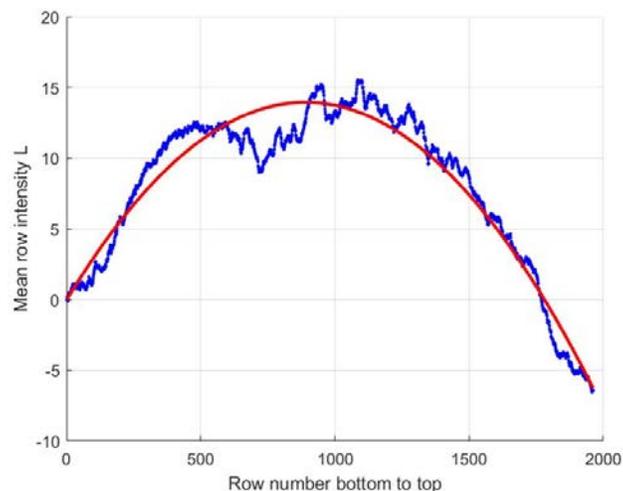

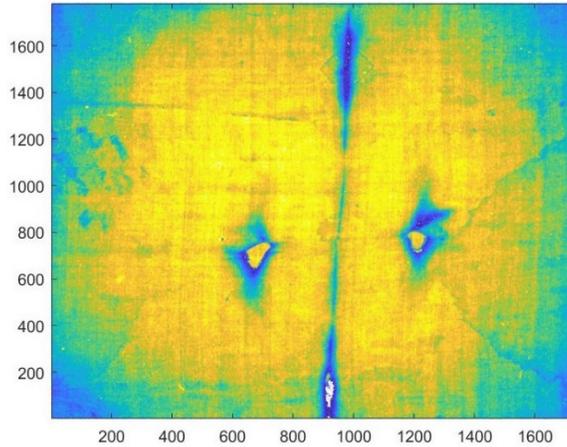Fig. 9. Plot of Average Row Intensity L from CIE L*a*b plot in Fig. 4

Fig. 10. Cropped image contour plot of intensity L for CIE L*a*b plot in Fig. 4

As can be seen the contour plot is much more symmetric than the original contour plot in Figure 4. The procedure discussed in this section was applied to all 16 uv images. In 7 of the 16 images burn marks made it difficult to achieve an illumination centered image using only the parabola approach. In these 7 cases additional cropping was carried out manually to determine the final illumination centered image. Table 1 gives the pixel sizes of the images that resulted.

Table 1. Pixel sizes of cropped illumination centered images

	Shroud top			Shroud bottom	
Image name	Row size	Column size	Image name	Row size	Column size
E3	1962	1619	B2	1962	1837
E6	1962	1518	B5	1762	1807
E8	962	1586	B9	1762	1832
E12	1782	1736	B12	1684	1684
E15	1785	1666	B15	1752	1782
E17	1772	1759	B17	1844	1777
E20	1862	1897	B20	1918	1846
E22	1878	1754	B22	1812	1815

In Table 1 the image names follow Miller's designation and that is why the first three names on the top and bottom have different numbers, i.e. E3 versus B2. The original E and B images in each row of Table 1 were directly opposite one another and they overlapped very slightly in the middle of the Shroud.

4.3 Detecting one outlier image

Contour plots for each of the cropped images in Table 1 were calculated and assembled into a composite plot for the entire Shroud shown in Figure 11.
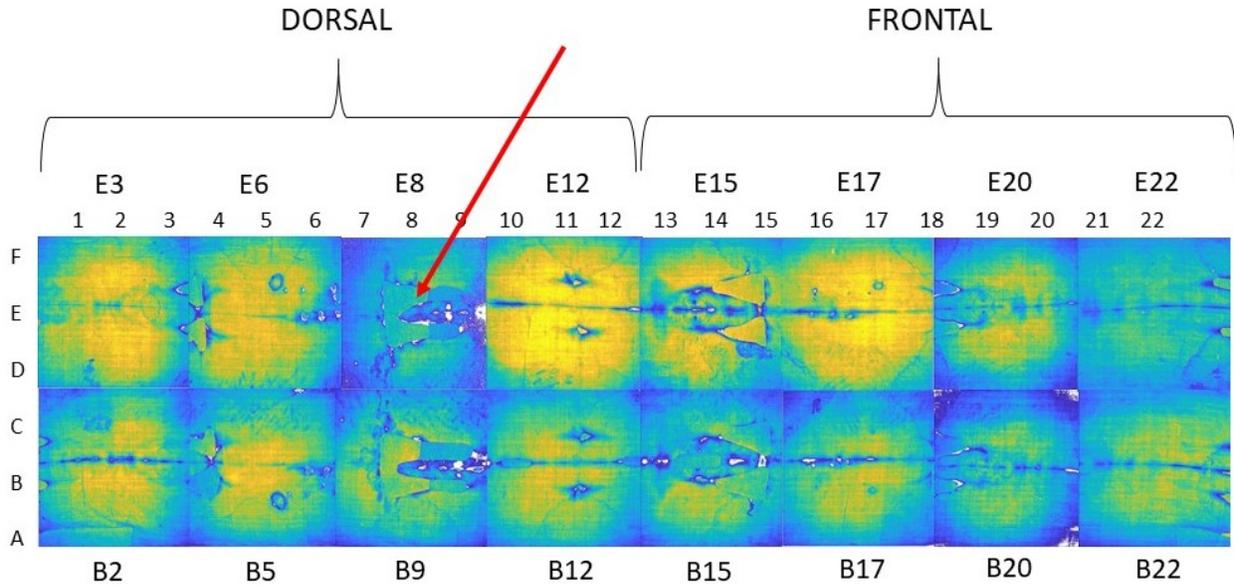
Fig. 11. Composite cropped contour plot of intensity L for the entire Shroud

The frontal image starts near the right side of E12, B12, and D12 below. Since there is more dorsal image in these 3 figures they are included in the dorsal image group. Before discussing the results in Figure 11, the issue of one outlier image needs to be addressed. The red arrow in Figure 11 points to this outlier image E8 which is shown in Figure 12.
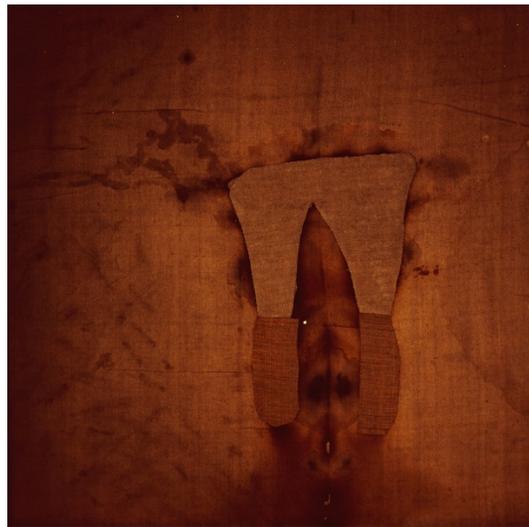

Fig. 12. Cropped Miller image (3c-UV-S1-E-8_0474 (E8)) [4] © Vernon Miller, 1978.

The image in Figure 12 is much darker and redder than the other 15 images that were downloaded. These other 15 images all look similar to Figure 2 in intensity and color. In addition to the 16 images studied in this section there are 28 other uv images on the website [4]. The images labeled E. UV light photos taken at burn marks, F. UV light photos taken at blood marks, and G. UV photos taken at burn and blood marks are all very similar to the image in Figure 12 in color and intensity [4]. Since Miller took his photos in 1978 and they were just published in 2019 it is possible that the image in Figure 12 was mislabeled.

The MATLAB® function isoutlier(A) was used to determine if any of the 16 images in Table 1 was an outlier. This routine returns a logical array whose elements are true when an outlier is detected in the corresponding element of A. By default, an outlier is a value that is more than three scaled median absolute deviations (MAD) away from the

median. The input to the isoutlier routine was the mean values of the CIE L*a*b color space representations of the 16 cropped contour images shown in Figure 11. The isoutlier routine indicated that E8 was an outlier based on it's CIE L*a*b a-color value. Image E8 was the only outlier detected and it is removed from the analysis below.

5. Discussion of cropped contoured intensity results

Figure 11 displays some very unusual fluorescence intensity properties. The mean intensities, L, for each of the 15 cropped images in Figure 11 are given in Table 2 together with their average values.

Table 2. CIE L*a*b intensities L of cropped and original images

	Shroud top (right)			Shroud bottom (left)	
Image name	Cropped intensity	Original intensity	Image name	Cropped intensity	Original intensity
E3	39.02	35.3	B2	33.47	32.43
E6	37.60	34.05	B5	33.32	30.7
E8	-	-	B9	29.89	27.56
E12	44.37	40.19	B12	34.49	30.01
E15	36.50	34.15	B15	29.73	27.47
E17	42.79	39.49	B17	31.64	29.36
E20	31.09	29.71	B20	29.17	24.53
E22	29.69	28.29	B22	32.62	31.92
Average	37.29	34.45	Average	31.79	29.14

Comparing the seven top and bottom images in Figure 11 it can be seen that the top images fluoresce more intensely in 6 of the 7 cases. Only B22 fluoresces more strongly than E22. To make sure that this effect was not caused by the cropping to center the illumination the means of the original 1962x1989 images before they were cropped to center the illumination were calculated. The assumption in calculating these means is that each of the original images would have approximately the same sized low illumination region in it. These means are listed in Table 2 as original intensities together with their average values. The correlation coefficients between the cropped and original intensities are .9945 for the top and .8639 for the bottom. The original intensities are also stronger for the top of the Shroud in the same 6 cases as the cropped intensities. The MATLAB® function ttest2 was used to check the equivalence of the averages given in Table 2. The ttest2 function implements Welch's method [26] for comparing means. Applying this test to the average of the 7 top cropped intensities compared to the 8 bottom cropped intensities shows that the means are not equal (p = .0197). The same test applied to the original intensities shows that their averages are not equal as well (p=.0125). These results lead to an important question: what would cause the top (right side) of the Shroud to fluoresce more strongly than the bottom (left side) of the Shroud.

Two other comparisons can be made, but they are limited by the burn marks in some of the 15 images. First the dorsal images near the feet fluoresce more than their frontal counterparts. Compare E3 to E22, E6 to E20, B2 to B22, and B5 to B20. Because of the extensive burn marks in images B8, B15, and E15 it is difficult to make a comparison between them and their counterparts B17, B12, and E12. For the cropped intensities the highest intensities occur at E12 and B12 which are near the image of the head on the Shroud. To achieve better comparisons a method to overcome the problems due to the burn marks is discussed next.

6. Overcoming the problem introduced by the burn marks

In addition to the 16 images analyzed above there are 6 additional uv images that Miller took that can be used to overcome the problems that the burn marks create. These 6 images were taken of the center of the Shroud, down the D C regions in Figure 5. The 6 images are labeled [4]: 2b-UV-S1-D-3_0454 (D3), 8-Misc.-UV-D-8_0508 (D8), 7a-UV-S3-D-12_0504 (D12), 7b-UV-S3-D-14 (D14)_0505, 7c-UV-S3-D-17_0507 (D17), and 2m-UV-S1-D-21_0467 (D21). The labels in parentheses are used below to designate these images. Five of these images have the label uv5 in their border and 1 uv4 (D3). The uv4 image may have been taken at a different time than the uv5 images. The f number for the 6 images is not given in [4], but it is given for the 16 images discussed above. The 6 images were cropped and resized to 1962x1989 as described in section 4.1 above. Figure 13 shows image D8.

Fig. 13. Cropped Miller image (8-Misc.-UV-D-8_0508 (D8)) [4] © Vernon Miller, 1978.

The image in Figure 13 was taken in the middle of the Shroud and it covers about ½ of the region that outlier image E8 shown in Figure 12 covers. It should be noted that the 6 D images do not cover the complete length of the Shroud because the image in one section between D17 and D21 is not given in [4]. There is an image (2d-UV-S1-D-6_0457) (D6) given in [4] for the region between D3 and D8. This image is extremely dark in color and similar to Figure 12 above. When D6 was cropped and resized 1962x1989 its mean CIE L*a*b intensity L was calculated as 16.11. One half of images E6 (left side) and B5 (right side) completely overlap image D6. Their mean intensity for the overlap regions was calculated as 30.03. The overlap regions for images E6 and B5 include the regions where they received the smallest amount of uv illumination. Based on the low intensity in image D6 it was concluded that this image was taken with a different exposure time than the other D images and it was eliminated from the discussion below.

A contour plot for the CIE L*a*b intensity L of the 6 images is shown in top half of Figure 14. The centering technique discussed in section 4.2 was not used on the 6 top images which all have a pixel size of 1962x1989.
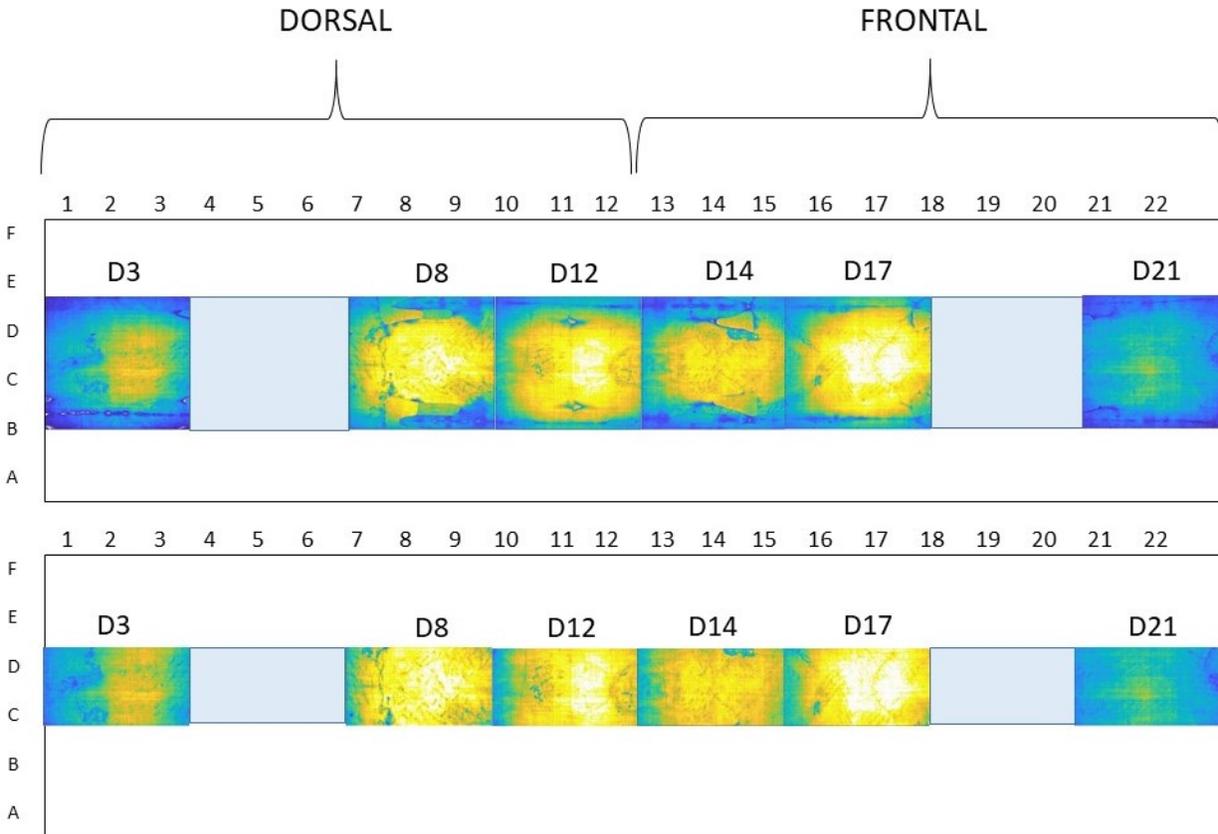
Fig. 14. Composite cropped contour plot of intensity L of 6 images for entire Shroud

The 2 gray boxes show where one image is missing and the other has been eliminated. Table 3 gives the mean values of the CIE L*a*b intensities L for the images in the top half of Figure 14.

Table 3. CIE L*a*b intensities L of images shown in Fig. 14

Image name	Intensity top half of Fig. 14	Intensity bottom half of Fig. 14
D3	30.13	36.60
D8	44.17	54.14
D12	45.09	52.68
D14	38.42	47.89
D17	47.16	55.32
D21	26.69	30.75

To eliminate the effects of burn marks the columns in the original CIE L*a*b images in the top half of Figure 14 were cropped from 1 to 1989 down to 500 to 1400, thereby eliminating all burn marks from the resulting images and the effects of the burn marks on image intensity. Then the mean intensities in the cropped images were recalculated and contoured. These contour plots are shown in the bottom half of Figure 14 and the resulting intensities are given in Table 3. From the intensities in the bottom half of Figure 14 the following conclusions can be drawn. The highest intensities are in images D8 and D17 which are near the center of the body image on the Shroud. The fluorescence intensity in the bottom half of Figure 14 drops off from the center of the body toward the head which is in regions D12 and D14. Comparing dorsal images D3 and D12 to their counterpart images D21 and D14 shows that these dorsal images fluoresce more than the frontal images. Frontal image D17 fluoresces slightly more than its counterpart dorsal image D8, 55.32 to 54.14. One explanation for this difference from the other 2 D comparisons could be that the image in D8 appears to have more scourge and blood marks than the image in D17. Blood marks would absorb fluorescence thereby reducing its reflected intensity. The intensities in the top half of Figure 14 can be compared with the original intensities in Table 2 since all these images have the same pixel size of 1962x1989. The center of the body image on

the Shroud which includes the area from the thighs up to the head fluorescence more than the images on either side of the Shroud. This result can be seen by comparing the intensities of D8, D12, D14, and D17 to the intensities of the images on either side of them, E12 to E17 and B9 to B17.

7. Summary of unique uv fluorescence properties of the Shroud

The following is a summary of the unique uv fluorescence properties of the Shroud:

1. uv fluorescence is highest in the mid-section of the image on the Shroud.
2. Except for the D17 D8 comparison the other six comparisons show that the dorsal side of the Shroud fluoresces more than the frontal side.
3. Six out of seven of the right hand sections of the Shroud (top) fluoresce more than the corresponding left hand sections (bottom).
4. uv fluorescence goes through a maximum near the mid-section of the image on the Shroud and it drops off somewhat toward the section with the head image and significantly toward the image of the feet.
5. The mid-section of the Shroud fluoresces more than the sides of the Shroud adjacent to the mid-section.

These uv fluorescence properties are unique and very interesting. An explanation for them is important in attempting to gain an understanding of the Shroud. An important question that should be addressed is: what could account for these unique uv fluorescence properties of the Shroud.

If neutron radiation affects the fluorescence properties of linen then this effect could explain the Shroud's unique uv fluorescence properties. Gilfillan and Linden [27] studied the effect of neutron irradiation on the strength of yarns, one of which was cotton. They hypothesized that neutron irradiation could cause proton recoil reactions in the fibers studied and that these reactions could affect cross linkage in the fibers. In their testing they used a large neutron fluence of 2.3×10^{17} neutrons/cm^2. This fluence was so large that it "practically destroyed the strength of the fiber [27]". In 2010 Lind, et al presented a paper [28] on the production of radiocarbon 14 (^{14}C) by neutron radiation of modern linen. The ^{14}C is produced from nitrogen 14 by neutron radiation. A sheet of unbleached modern plain-woven flax linen, which measured 0.99 m in the warp direction by 1.56 m in the weft direction, was used in their study. Lind et al used a neutron fluence of 1.07×10^{14} n·cm^{-2} which was calculated to produce a quantity of ^{14}C that would be equal that which would be required to change the radiocarbon Shroud date from 33 to 1260 to 1390. The authors provided two pieces of their neutron irradiated linen together with two pieces of non-irradiated control linen to the author for this study. When this linen was photographed with a uv camera no difference in fluorescence intensity was detected. One control and one irradiated piece of linen were also heated at 180 °C for 3 hours to artificially age them. After heating the neutron irradiated sample had a slightly lower fluorescence intensity than the control piece. The difference between the 2 fluences in these 2 studies [27,28] is over 3 orders of magnitude. At the high end fiber is almost destroyed and at the low end no increase in fluorescence intensity is seen. Whether fluorescence intensity changes at fluences between these 2 extremes is an open question. In the next section it is assumed that uv fluorescence could be affected by neutron radiation. In the Summary and future work section an experiment is proposed to evaluate this assumption.

8. MCNP simulation of neutron radiation from the body wrapped in the Shroud

At the 2014 St. Louis Shroud Conference Robert Rucker gave a presentation entitled:" MCNP Analysis of Neutrons Released from Jesus' Body in the Resurrection". A very detailed description of Rucker's simulation method is given on his website [20]. Rucker was interested in following up on the suggestion made by Phillips [12] that neutron radiation could have altered the radiocarbon content of the Shroud, and therefore its radiocarbon date. He used a computer software package [21], MCNP (Monte Carlo Neutron Particle) that was developed at the Los Alamos National Laboratory to simulate neutron emissions. Rucker developed a very detailed geometric model of a tomb that would have existed in the first century AD. He states that the main assumption in his simulation is: "that the thermal neutrons were emitted homogeneously (uniformly) from within the body and isotropically (uniformly) in all directions, so that the same number of neutrons would be emitted from every volume, i.e. every cm^3, within the body." Rucker's simulation calculated how emitted neutrons from the body would have affected the radiocarbon dating of

the Shroud. Thus his results give predicted radiocarbon dating ages for various parts of the Shroud. His simulation matched the 1260AD radiocarbon date determined in 1988 [5] for the corner of the Shroud tested. His simulation also had a slope of radiocarbon dates that matched that of the three laboratories that carried out the radiocarbon dating of the Shroud. Much more information is given in [20]. It can be noted that Rucker's simulation predicts that areas of the Shroud would date to the future because of the effects of neutron radiation. If additional radiocarbon testing of the Shroud is carried out this prediction could be tested.

Neutrons are known to affect the radiocarbon date of linen [28]. If neutrons affect uv fluorescence then there should be a correlation between radiocarbon dates and uv fluorescence. Rucker's simulation resulted in radiocarbon dates for numerous parts of the Shroud. The following are Rucker's very interesting key conclusions about radiocarbon dating of areas of the Shroud [20]:

1. "The values (radiocarbon dates) are higher near the elbows than near the knees because the elbows are closer to the center of the body mass and so would be closer to where more neutrons would be emitted, assuming the neutrons are emitted homogeneously (uniformly) from the body. "

2. "The values (radiocarbon dates) are higher near the back (dorsal) image than near the front image because neutrons reflected from the limestone bench below the dorsal half of the cloth would have caused a higher fraction of the neutrons to pass through the dorsal half of the cloth multiple times, thus causing a greater shift in the predicted dates."

3. "The values (radiocarbon dates) on the right side of the image are higher than on the left side of the image because the locations on the right side of the image would have been closer to the back wall of the tomb, assuming the head was toward the right side as the body lay on the back bench in the tomb. This is because neutron reflection from the limestone wall at the back of the tomb would have caused a higher fraction of the neutrons to pass through the right side of the cloth multiple times, thus causing a greater shift in the predicted dates."

If one takes Rucker's conclusions and substitutes uv fluorescence intensity for radiocarbon dating values they line up very closely with the summary of uv fluorescence properties given in section 7 above. Compare conclusions 1 to 3 in section 7 with Rucker's key conclusions 1 to 3. Rucker also gives plots that show a drop off in predicted radiocarbon age near the head image, which agrees with conclusion 4 in section 7. Similarly Rucker gives plots that show that radiocarbon dates would drop off from the center of the torso toward both sides of the Shroud in agreement with conclusion 5 in section 7.

Neutron radiation may not be the cause of the unique uv fluorescence properties of the Shroud of Turin. In that case an alternative explanation that accounts for these unique properties should be proposed. The following section suggests additional experiments that can be performed as a follow up to the results presented here.

9. Summary and future research

This paper has examined recently published uv images of the Shroud of Turin. A method to overcome the uneven illumination problem with these images is presented. It has been shown that the Shroud of Turin exhibits very unique uv fluorescence properties which are summarized in section 7.

Several fruitful areas of follow up research to the work presented here can be suggested. First, to check the assumption that neutron irradiation affects uv fluorescence modern linen could be irradiated with several neutron fluences. The fluence values to be tried could be determined from Rucker's simulation [20]. Once irradiated the modern linen could be photographed using a uv light source to determine if uv intensity changed with neutron exposure. Irradiated samples could be compared to non-irradiated control samples. Also, the effect of neutron radiation on uv fluorescence could take time to occur. Thus, any modern linen studied should be artificially aged by heating and then checked for uv fluorescence as well.

Second, it would also be useful if methods for estimating the uneven illumination in Vern Miller's photos could be developed. One approach would be to duplicate Miller's uv lighting set up shown in Figure 1. Then uv photos

could be taken of a blank linen sheet and the resulting intensity determined. Once determined this intensity could be divided into that of Miller's images to remove the uneven illumination in them. Another possible approach would be to develop a first principles model of uv illumination based on the physics of light for the set up in Figure 1. Lastly, there may be data based approaches that could be used to estimate the illumination pattern directly from the data in Miller's uv photos. If a method to estimate the uneven illumination can be developed it would have to be applied to the center point of the illumination in Miller's images. The method given in Section 4.2 is one method of determining the center of illumination. There may be additional, better approaches to this problem that can be developed.

The best approach to follow up on this study would be to take new uv photos of the Shroud using a uniform lighting source. Finally, carrying out additional radiocarbon dating from several Shroud sites would greatly help clarify mysteries of the Shroud.

Acknowledgements

References

1. https://www.shroud.com/78strp10.htm.
2. V.D. Miller, and S.F. Pellicori, "Ultraviolet fluorescence photography of the Shroud of Turin," Journal of Biological Photography, **49**(3), 71-85 (1981).
3. D. Devan, D. and V. Miller, "Quantitative photography of the Shroud of Turin," IEEE 1982 Proceedings of the International Conference on Cybernetics and Society, 548-553 (1982).
4. https://www.shroudphotos.com/
5. P. E. Damon, D. J. Donahue, B. H. Gore, A. L. Hatheway, A. J. T. Jull, T. W. Linick, P. J. Sercel, L. J. Toolin, C.R. Bronk, E. T. Hall, R. E. M. Hedges, R. Housley, I. A. Law, C. Perry, G. Bonani, S. Trumbore, W. Woelfli, J. C. Ambers, S. G. E. Bowman, M. N. Leese and M. S. Tite, **"**Radiocarbon dating of the Shroud of Turin"*Nature***,** 337 (6208), 611-615, (1989).
6. R. Van Haelst, " Radiocarbon dating the Shroud: a critical statistical analysis", available at https://www.shroud.com/ vanhels3.htm (1997).
7. T. Casabianca, E. Marinelli, G. Pernagallo, and B. Torrisi, "Carbon dating of the Turin Shroud: New evidence from raw data," Archaeometry, in press (2019).
8. G. Fanti, G. Baraldi, P. Basso, R. Tinti, "A Non-destructive dating of ancient flax textiles by means of vibrational spectroscopy, " Vibrational Spectroscopy, 67, 61–70 (2013).
9. Fanti, G., and Malfi, P., "Multi-parametric micro-mechanical dating of single-fibers coming from ancient flax textiles," Textile Research Journal, 84, 714–27 (2014).
10. H.E. Gove, "Dating the Shroud of Turin – an assessment," Radiocarbon, 32 (1), 87-92 (1990).
11. R. Rucker, "Carbon dating of the Shroud of Turin to 1260-1390 AD is not explained by normal contamination," http://www.shroudresearch.net/
12. T. J. Phillips, "Shroud irradiated with neutrons?," Nature, 337 (16), 594 (1989).
13. J. B. Rinaudo, "Nouveau mécanisme de formation de l'image sur le Linceul de Turin, ayant pu entraîner une fausse radiodatation médiévale", L'Identification Scientifique de l'Homme du Linceul, Jésus de Nazareth, Actes du Symposium Scientifique International, Rome 1993, F.-X. De Guibert Editor, Paris, 293-299 (1995).
14. J. Rinaudo, "Protonic model of image formation on the Shroud of Turin," Third International Congress on the Shroud of Turin, Turin, Italy, June 5-7 (1998).
15. J. P. Jackson, "Is the image on the Shroud due to a process heretofore unknown to modern science?," The International Scientific Symposium, Paris, France, 1-29 (1989).
16. J. P. Jackson, https://www.shroudofturin.com/Resources/ShroudForwardtoFallThrough.pdf
17. M. Antonacci, "Particle radiation from the body could explain the Shroud's images and its carbon dating", Scientific Research and Essays 7(29), 2613-2623 (2012).
18. M. Antonacci, Test The Shroud, Forefront Publishing Co., St. Louis, MO, Chapters 5, 6, 11, and 12, (2015).
19. Ibid. Chapter 7.
20. R. Rucker, "The Carbon Dating Problem for the Shroud of Turin, Part 3: The Neutron Absorption Hypothesis", http://www.shroudresearch.net/
21. MCNP6 User's Manual -Code Version 6.1.1beta, LA-CP-14-0074, June 2014, Los Alamos National Laboratory (LANL), Los Alamos, New Mexico.
22. CIE L*a*b Color Space, https://en.wikipedia.org/wiki/CIELAB_color_space.
23. T. McAvoy, "Image processing applied to uv photo of the Shroud of Turin which includes the radiocarbon test area," submitted to Scientific Research and Essays, May (2019).
24. https://www.mathworks.com/
25. C. Avis, D. Lynn, J. Lorre, S. Lavoie, J. Clark, E. Armstrong, J. Addington, "Image processing of the Shroud of Turin," Proceedings of the IEEE International Conference on Cybernetics and Society, 554-558. (1982).

26. B.L. Welch, "The generalization of "Student's" problem when several different population variances are involved ", <u>Biometrika</u>, 34(1), 28-35 (1947).

27. E.S.Gilfillan, "Effects of nuclear radiation on the strength of yarn," Textile Research Journal, 25(9), 773-777 (1955).

28. A. C. Lind, M. Antonacci, G. Fanti, D. Elmore, and J. M. Guthrie, "Production of radiocarbon by neutron radiation on linen," Proceedings of the International Workshop on the Scientific approach to the Acheiropoietos Images, ENEA Frascati, Italy, 4-6 May (2010). http://www.acheiropoietos.info/proceedings/LindWeb.pdf